Landfast Sea Ice Extent and Variability in the Alaskan Arctic Derived From SAR Imagery

Andy Mahoney[1], Hajo Eicken[1], Allison Graves[2], Lew Shapiro[1] and Patrick Cotter[1]
mahoney@gi.alaska.edu, eicken@gi.alaska.edu, Nunatech@usa.net, Lews@gi.alaska.edu, pcotter@gi.alaska.edu

[1]Geophysical Institute, University of Alaska Fairbanks, Fairbanks, AK 99775
[2]Nuna Technologies, PO Box 1483 Homer, AK 99603

1 Introduction

Landfast sea ice is a seasonal phenomena in the Alaskan Arctic and throughout its annual existence, between formation in late fall and break-up in late spring, it is shaped by a range of thermodynamic and dynamic forces (Barnes *et al.* 1979; Shapiro and Metzner, 1989). The most apparent changes are those in landfast ice area and extent when floes of ice attach to and break off from its seaward edge. The position of the seaward landfast ice edge (SLIE) over the course of the year generally advances offshore to a stable position in mid-winter before retreating with the onset of spring. However, higher frequency changes in position also occur on timescales of days to weeks, which are generally small but occasionally affect the full width of the landfast ice. The location and stability of the SLIE at any point in time affects the activities of people and wildlife in the coastal arctic as it marks the boundary between stationary, continuous sea ice and drifting deforming pack ice. It is a vital consideration for people hunting or working on the ice in determining where food sources might be or where spilt oil might go. Since landfast ice occupies the shallowest water in the arctic, its presence or absence is also important for coastal process such as erosion and sediment entrainment.

Here we present results of a manual and an automated technique to derive positions of the seaward landfast ice edge (SLIE) as it changes over time from synthetic aperture radar (SAR) data covering the Alaskan Arctic coast and nearshore waters from east of Point Lay, Alaska to the Mackenzie delta. Observing the variability in the position of the SLIE for a large study area over the course of the year identifies the occurrences of significant change including the timing of freeze-up and break-up and episodic events in between. It is also possible to identify the maximum stable extent of the landfast ice for a given period, which should prove valuable for all nearshore activity in the Arctic. We can gain a greater understanding of the factors controlling the SLIE position by calculating of the standard deviation in landfast ice width along the coast. This analysis identifies stable nodes along the SLIE where variability is small and processes, as of yet unidentified, help stabilize the landfast ice edge.

2 Method

The identification of sea ice in SAR imagery is not a straightforward task, since a similar range of backscatter amplitudes can be received from ice and open water surfaces, depending on surface roughness characteristics. Furthermore, the definition of landfast implies stability over a given period of time, meaning that a single image is insufficient to determine what is landfast ice and what is drifting pack ice. Applying this definition, however, it is possible to identify landfast ice from a sequence of calibrated colocated SAR scenes as those parts of the imagery over the ocean and adjacent to the land that exhibit some component of stability or no change.

Subtraction and cross-correlation of colocated image pairs did not yield accurate results unless a coastal flaw lead between the landfast and drifting pack ice was present. Principal component analysis of a sequence of 3 or 4 consecutive scenes provided better results and was able to distinguish the SLIE even when there was no coastal flaw lead present, but did not perform well when the backscatter between subsequent scenes differed significantly due to differences in incidence angle and other environmental changes of the ice surface.

0-7803-8742-2/04/$20.00 (c) 2004 IEEE

The features of the image that exhibit most spatial consistency over time are linear regions of high backscatter, most likely related to zones of ridges on the ice surface, which may or may not be grounded. These regions are typically a few hundred meters wide and parallel or sub-parallel with the coast. A technique for distinguishing landfast ice must therefore be able to recognize these features and their orientation. There are a number of edge detection algorithms that will highlight these features, but the value returned at a given point does not hold any information about the orientation of the overall feature.

The 2 dimensional vector gradient of a scalar is given by:

$$\nabla\Phi = \frac{\partial\Phi}{\partial x}\underline{i} + \frac{\partial\Phi}{\partial y}\underline{j} \quad (1)$$

This can be approximated with finite differences for a digital grayscale image as

$$\nabla\Phi_{x,y} \approx \frac{\Phi_{x-d,y} - \Phi_{x+d,y}}{d}\ \underline{i} + \frac{\Phi_{x,y-d} - \Phi_{x,y+d}}{d}\ \underline{j} \quad (2)$$

where $\underline{i}$ and j are horizontal and vertical unit vectors in the image plane and x and y are the image co-ordinates.

By calculating the vector spatial grayscale gradient field of the images we generate two images that represent the horizontal and vertical components of the gradient field. From these it is possible to characterize features by both the magnitude and direction of the gradient. This is demonstrated in Figure 1. Note the orientation of features in the two gradient component images.

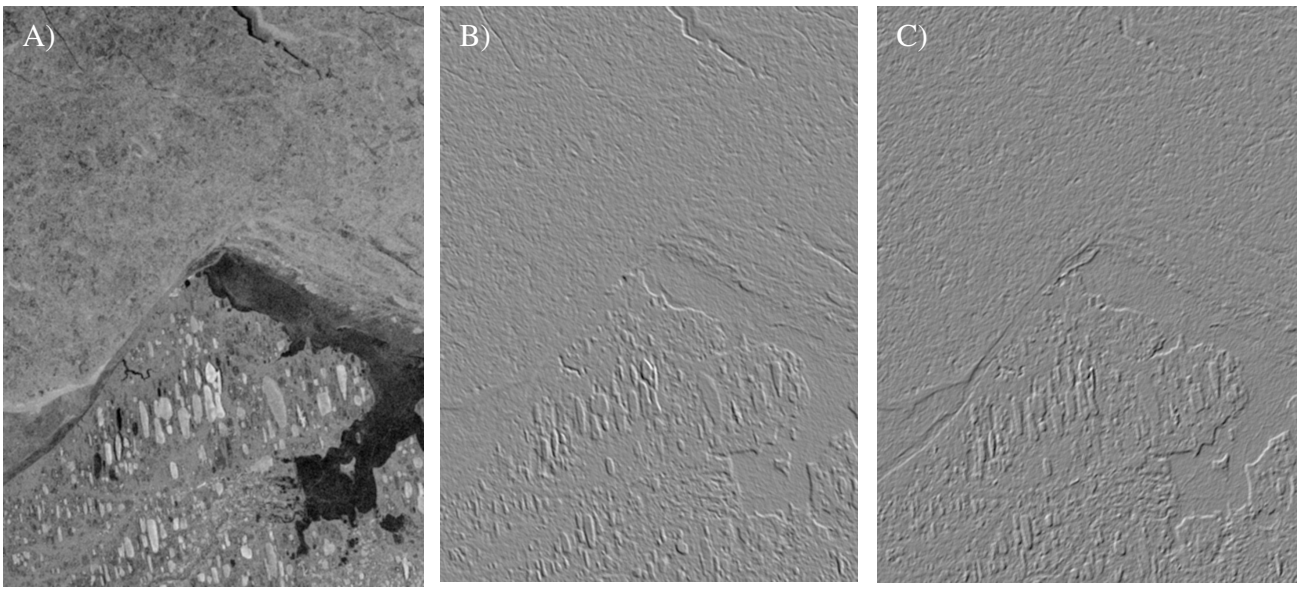

Figure 1: a) Calibrated Radarsat ScanSAR image over Barrow, Alaska Jan 6 2002. Smoothed by 5 pixel (500m) filter, b) Horizontal component of grayscale gradient field, c) Vertical component of grayscale gradient field. Bright areas are positive gradients and dark areas are negative gradients, with axes positive to the right and downwards. Note how features have different orientations in the horizontal and vertical component images

Thus by calculating the net gradient difference for each component between consecutive images we can distinguish between features with different orientations, as illustrated in Figure 2. The calculation for the horizontal gradient component is described by:

$$\Delta_{net}\nabla_H = \left|\nabla_H\Phi_1 - \nabla_H\Phi_2\right| + \left|\nabla_H\Phi_1 - \nabla_H\Phi_3\right| + \left|\nabla_H\Phi_2 - \nabla_H\Phi_3\right| \quad (3)$$

Where Φ_1, Φ_2 and Φ_3 are the 3 consecutive grayscale images and ∇_H is the horizontal gradient component.

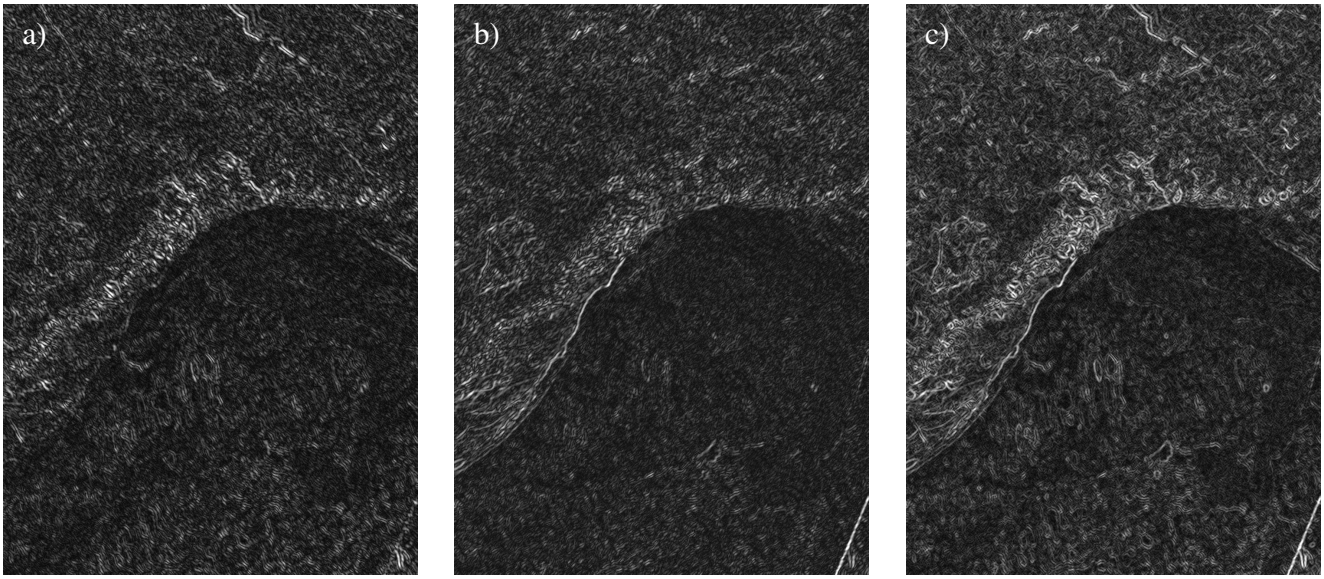

Figure 2: The net difference between gradient fields of 3 consecutive Radarsat images of Barrow on Jan 6, 16 and 20 2002. a) Net difference in horizontal components. b) Net difference in vertical components. c) Magnitude of horizontal and vertical components. The landfast is characterized by dark regions of low gradient difference adjacent to the land and typically bounded by bright, linear regions of high gradient difference.

Figure 3: The thresholded gradient difference image from Figure 2c, with the coast mask overlain.

In the magnitude image of the two components of the gradient difference (Figure 2c), the landfast ice occupies the dark region of low gradient difference values adjacent to the coast. The SLIE is identified by bright regions of high gradient difference. Thresholding the image at a gray value corresponding to a net backscatter gradient difference of 8 dB / km the SLIE becomes easy to see (Figure 3) and can be manually delineated. A technique for automatically delineating the SLIE from the gradient difference images proves elusive at this time, since the SLIE can sometimes be less distinct in some areas and bright regions sometimes occur along the coast particularly in springtime when surface flooding from rivers occurs.

These images of Barrow represent the coverage of one of ten subregions into which the whole study area was divided in order to obtain images free from mosaicking edges prior to calculating the gradient fields. Continuous SLIE's for the whole study area were produced by mosaicking the subregions back together. For the manual technique, full mosaics not made up from subregions were examined. For consistency with the automated technique, 3 consecutive images were considered and the SLIE was drawn bounding areas in which no movement of features was apparent in all 3 mosaics.

3 Results

33 complete mosaics covering the study region were obtained for the period from October 31 2001 to July 9 2002. Each mosaic was comprised of images typically spanning 2 or 3 days, but in some cases 5 days where imagery was not available. The average period between mosaics was 8 days. By considering 3 consecutive mosaics at a time, 31 SLIE's were delineated with an average time period represented by each of 17 days. This was the same for both the automated and manual delineation techniques.

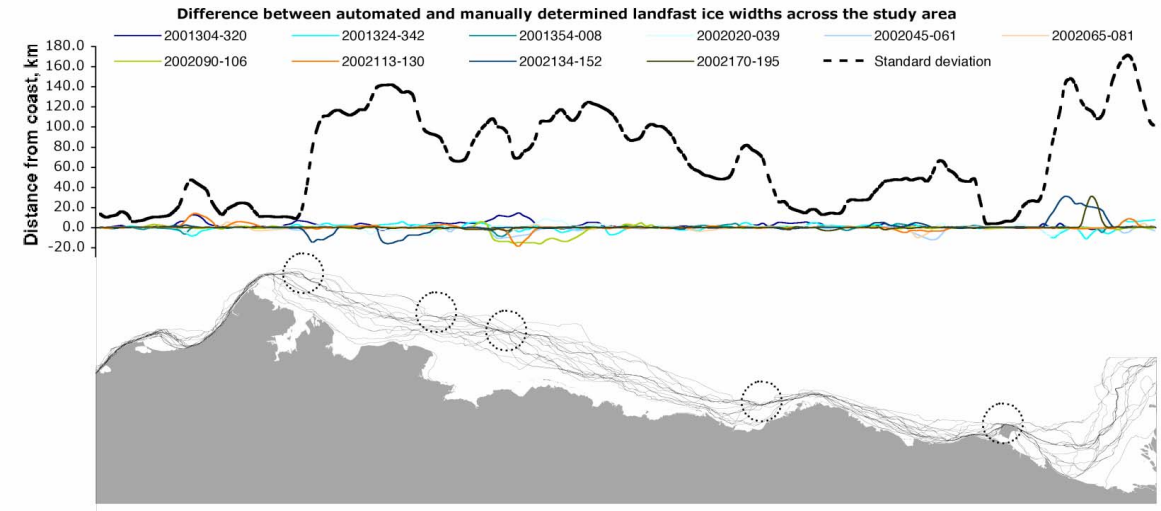

Figure 4: The seaward landfast ice edges (SLIE's) delineated from 31 gradient difference images for the whole study region from east of Point Lay to the Mackenzie Delta. See text for explanation.

All 31 SLIE's determined from the automated technique are shown in Figure 4. From this picture, regions of high variability and nodes of stability (shown by dotted circles) can be seen. Also plotted in Figure 4 are the differences in landfast ice width between the automated and manual techniques for 10 SLIE's and the standard deviations determined from all the automated SLIE's. Each difference curve is identified by the year and day of year range of the 3 mosaics it is determined from. All curves are plotted to scale with the coast. The fast ice widths are measured along a curvilinear co-ordinate system, sub-parallel to the coast, but it can be seen that the stable nodes align with regions of low standard deviation and the regions of greatest difference between the two techniques align with regions of high standard deviation.

4 Discussion

In determining the position of SLIE's though the year, agreement between the two techniques is good, especially when compared with the standard deviation of landfast ice width along the coast for the whole year. Although to some extent the results of automated technique was being checked against those derived manually, it should be pointed out that the manual technique contains a higher degree of subjectivity. On occasion two different operators derived SLIE's from the same data with greater differences than when compared with the automated technique. Extra confidence is given to the results of the automated technique by the identification of stable nodes. Although all processes giving rise to these features are not known, they are perhaps to have been expected. Future work will integrate bathymetric data, larger scale ice motion and lead patterns to the analysis.

Both the manual and automated techniques captured the seasonal cycle of the landfast ice development and break-up through the sea ice season 2001-02. Dates of formation and break-up and episodic events in between can be determined, though these results will be of more use later when more years of SAR data have been examined. Although a detailed analysis has not been made, the early spring maximum fast ice extent is consistent with those determined for the early 1970's by Barry et al. (1979). With seven more years of Radarsat data available between 1996 and 2004, the techniques presented here for delineating the SLIE positions throughout those years hold promise for assessing changes in the landfast ice regimes of the Alaskan Arctic and helping elucidate the processes responsible.

References

Barry, R, R.E. Moritz and J.C. Rogers, 1979, The Fast Ice Regimes of the Beaufort and Chukchi Sea Coasts, Alaska, *Cold Regions Science and Technology*, **1**, pp 129-152

Shapiro, L.H and R.C. Metzner, 1989, Nearshore Ice Conditions from Radar Data, Point Barrow Area, Alaska, *Geophysical Institute Report UAG-R(132)*